structure at low energies. A novel feature of the model is that it allows the calculation of both bound and continuum states from the same forces. In the light of the demonstrated sensitivity of the resonance structure to the residual interaction and to the dimensionality of the shell-model space, the choice of these components of the model deserves more detailed investigation. We are currently considering these questions and are also investigating the physical content of the resulting wave functions.

We gratefully acknowledge the use of the Oak Ridge National Laboratory–University of Rochester shell-model code[14] and a structure-coefficient tape kindly prepared for us by Edith Halbert.

†Work supported in part by the National Science Foundation under Grants No. NSF-GP-15855, No. NSF-GJ-367, and No. NSF-GU-2612.

[1]C. H. Johnson, Phys. Rev. C 7, 561 (1973).
[2]C. B. Dover and N. Van Giai, Nucl. Phys. A177, 559 (1971).
[3]A. D. MacKellar, J. F. Reading, and A. K. Kerman, Phys. Rev. C 3, 460 (1971).
[4]R. J. Philpott, Phys. Rev. C 5, 1457 (1972).
[5]P. Ferenman, in *Cargese Lectures in Physics*, edited by M. Jean (Gordon and Breach, New York, 1969), Vol. 3, and references therein.
[6]A. P. Zuker, B. Buck, and J. B. McGrory, Phys. Rev. Lett. 21, 39 (1968).
[7]I. Unna and I. Talmi, Phys. Rev. 112, 452 (1958).
[8]R. J. Philpott, Phys. Rev. C 7, 869 (1973).
[9]R. J. Philpott, Nucl. Phys. A208, 236 (1973).
[10]A. P. Zuker, Phys. Rev. Lett. 23, 983 (1969).
[11]W. W. True, Phys. Rev. 130, 1530 (1963).
[12]H. Crannel, Phys. Rev. 148, 1107 (1966).
[13]I. Sick and J. S. McCarthy, Nucl. Phys. A150, 631 (1970).
[14]J. B. French, E. C. Halbert, J. B. McGrory, and S. S. M. Wong, in *Advances in Nuclear Physics*, edited by M. Baranger and E. Vogt (Plenum, New York, 1969).

Systematic Study of $K^{\pm}$ Charge Exchange from 3 to 6 GeV/c*

R. Diebold, D. S. Ayres, A. F. Greene,† S. L. Kramer, A. J. Pawlicki, and A. B. Wicklund
Argonne National Laboratory, Argonne, Illinois 60439
(Received 19 February 1974)

Differential cross sections for $K^-p \to \bar{K}^0 n$ and $K^+n \to K^0 p$ have been measured at 3, 4, and 6 GeV/c using a data sample of 6000 events. Contrary to simple exchange-degenerate models, the ratio of K^+ to K^- cross sections was found to be approximately 1.35, with little dependence on either s or t. Both reactions show a shallow dip near the forward direction, suggesting the importance of spin-flip amplitudes.

The reactions

$$K^-p \to \bar{K}^0 n, \tag{1}$$

$$K^-d \to \bar{K}^0 nn, \tag{2}$$

$$K^+d \to K^0 pp \tag{3}$$

were observed with the Argonne effective-mass spectrometer for $|t| \leq 1.2$ GeV^2 at 3, 4, and 6 GeV/c. The spectrometer, consisting of a large dipole magnet surrounded by magnetostrictive wire spark chambers, has been described previously.[1] Only the incident beam particle and the pions from the K^0 decay were detected.

This experiment is the first detailed study of the relative energy dependence of the two charge-exchange reactions, with data at three energies for both K^- and K^+ reactions. The numbers of events are shown in Table I. The data sample for Reaction (3) contains more than twice the number of events collected by all previous experiments above 2 GeV/c.

Reactions (2) and (3) are closely related by line reversal, with differences between them due to interference of amplitudes with opposite C parity in the t channel. The dominant exchanges are thought to be the ρ and A_2 trajectories, having opposite C parity. If these trajectories are degenerate, as suggested by the ρ and A_2 masses and by duality arguments, the amplitudes would be 90° out of phase, and the two cross sections would be identical.[2] Our data show that this simple model is inadequate since the K^+ cross sections are consistently higher than the K^- cross sections.

The basic trigger for the experiment was an incident $K^{\pm}$, an interaction in the 20-in. target,

TABLE I. Numbers of events after all cuts were made and the resulting differential cross sections. The factors used to convert from deuterium to free-nucleon cross sections are shown in the last column. The total cross sections were obtained by integration of $d\sigma/dt$ from 0 to 1.2 GeV^2 (0 to 0.8 GeV^2 at 3 GeV/c); corrections were made for the contributions at larger t (typically 12%, estimated from bubble-chamber data). The results of two fits are shown; see text for details. The χ^2 values are for seven degrees of freedom. The errors shown are mainly statistical and do not include the estimated ± 8% uncertainty in absolute cross section.

		$K^-p \to \bar{K}^0n$			$K^+n \to K^0p$			
	p_{lab}(GeV/c)	3	4	6	3	4	6	Deuterium Correction
	Events	652	1738	760	680	1907	918	
$\frac{d\sigma}{dt}$ (μb/GeV^2)	-t = .01	980 ± 140	540 ± 60	290 ± 80	920 ± 180	740 ± 100	430 ± 110	.42
	.04	940 ± 100	650 ± 40	360 ± 50	1070 ± 110	720 ± 50	450 ± 50	.77
	.09	930 ± 80	570 ± 36	430 ± 40	1300 ± 110	860 ± 50	460 ± 40	.89
	.16	930 ± 90	572 ± 33	292 ± 25	1200 ± 110	850 ± 40	454 ± 30	.94
	.25	680 ± 90	484 ± 32	264 ± 24	1030 ± 120	630 ± 40	316 ± 26	.95
	.35	560 ± 100	358 ± 34	163 ± 19	830 ± 130	490 ± 40	175 ± 20	.96
	.45	300 ± 90	220 ± 29	59 ± 14	830 ± 170	284 ± 35	111 ± 16	.96
	.55	180 ± 80	143 ± 27	78 ± 15	520 ± 150	214 ± 34	85 ± 15	.97
	.70	430 ± 120	63 ± 13	34 ± 8	240 ± 130	119 ± 26	45 ± 10	.97
	.90	300 ± 140	44 ± 14	25 ± 8		85 ± 43	25 ± 9	.97
	1.10		56 ± 17	7 ± 6		28 ± 27	13 ± 10	.97
	1.30		20 ± 12	10 ± 6			20 ± 14	.97
	σ_{tot} (μb)	570 ± 50	300 ± 14	150 ± 8	697 ± 54	403 ± 20	188 ± 10	
Bessel Fit (eq. 5)	$(d\sigma/dt)_0$	1010 ± 100	540 ± 40	400 ± 50	950 ± 130	680 ± 60	480 ± 60	
	R_0	8 ± 2	13 ± 2	10 ± 2	13 ± 3	14 ± 2	11 ± 2	
	B	-.1 ± .4	.9 ± .2	1.5 ± .3	-.3 ± .5	.8 ± .2	1.5 ± .2	
	χ^2	9	4	18	3	7	8	
$(a_0+a_1t)e^{Bt}$ (eq. 6)	$(d\sigma/dt)_0$	960 ± 120	530 ± 50	330 ± 60	890 ± 150	610 ± 80	420 ± 70	
	R_0	6 ± 3	11 ± 3	12 ± 5	12 ± 5	16 ± 4	11 ± 4	
	B	4.8 ± .9	5.9 ± .3	6.8 ± .5	4.9 ± .6	6.1 ± .3	6.6 ± .5	
	χ^2	11	7	20	2	6	9	

two or more particles in the hodoscope at the spectrometer exit, and no counts in the veto counters which lined the magnet aperture. No neutral-link requirement was made, allowing some background from processes such as $K^-p \to K^-\pi^+n$. This background was suppressed by a factor of 2 by rejecting events which gave an effective $K\pi$ mass near the $K^*(890)$.

Missing-mass distributions were used to isolate the reactions of interest, the nucleon peak being well separated from inelastic events with pion production; see Fig. 1(a). Even for the deuterium target this missing mass was calculated as if the reaction took place from a free nucleon. As shown by the figure, Fermi-momentum smearing does not seriously affect identification of the reaction. Cutting on $M_X^2 < 1.09$ GeV^2 yielded the $M_{\pi\pi}$ distribution of Fig. 1(b). A cut on $M_{\pi\pi}$ from 488 to 506 MeV was used to calculate cross sections; the background in this interval was typically 10% and was corrected bin by bin by subtracting events in control regions.

A Monte Carlo program was used to correct for decays outside the fiducial region (typically 40%) as well as for events lost because of interactions in the target (about 5% for hydrogen, 10% for deuterium), pion decay in the spectrometer (about 5%), the cut on K^* mass (15%), and geometric acceptance (typically 50%). Corrections were also made for losses from the M_X^2 and $M_{\pi\pi}$ cuts, interactions in the spectrometer (5%), reconstruction losses (7%), decays of the $K^\pm$ beam before the target (3%), empty-target background (1%), and rate effects (3%). A branching ratio $(K^0 \to \pi^+\pi^-)/(K^0 \to \text{all})$ of 0.344 was used. The overall normalization uncertainty is estimated to be ± 8% and has not been included in the errors shown in the table and figures. The relative normalization uncertainty for the $K^\pm$ cross sections is ± 4%.

One further relative uncertainty between the K^- and K^+ reactions is related to the veto counters which lined the front half of the magnet aperture.

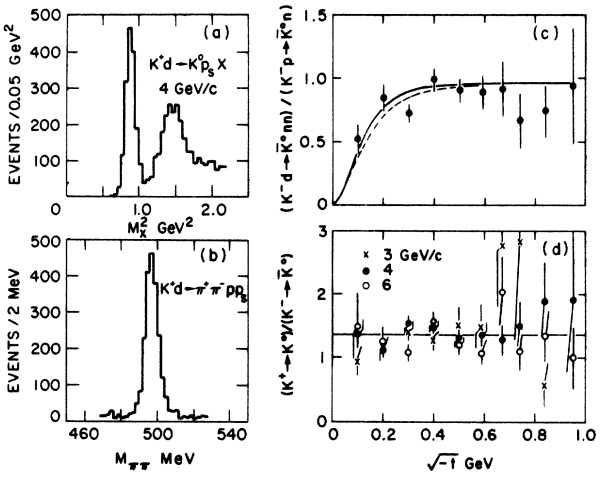

FIG. 1. (a) Missing mass calculated by ignoring the spectator proton. The distribution has been corrected for non-K^0 events by a sideband subtraction. (b) Mass distribution showing the K^0 signal for events with $M_X^2 < 1.09$ GeV^2. (c) Ratio of K^- charge-exchange cross sections from deuterium and hydrogen averaged over the three laboratory momenta. Solid line, $f(t)$ [Eq. (4)] for $R = 14|t|$; dashed line, for $R = 0$. (d) Ratio of K^+ to K^- charge-exchange cross sections. For reference, a line at 1.35 is shown.

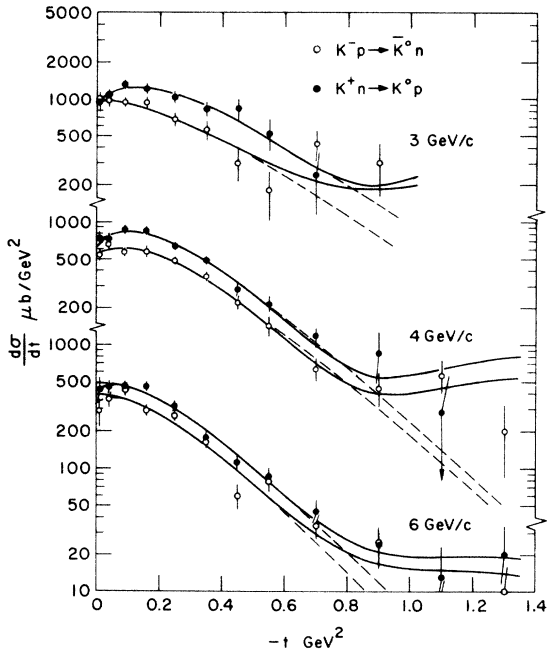

FIG. 2. Results of this experiment corrected to free-nucleon targets. Solid curves, Bessel-function fits to the data from 0 to 1.0 GeV^2; dashed curves, results of fits by Eq. (6) in regions where the two fits differ.

Monte Carlo studies, verified by experimental tests, showed that at large t these counters rejected some of the recoil protons from the K^+ reaction.[3] An uncertainty of $\pm\frac{1}{3}$ of the correction was added quadratically to the statistical error for this reaction.

It was assumed that relative to a free-nucleon target the deuterium cross sections were suppressed by the factor[4]

$$f(t) = 0.97\{[1 - S(t)] + R[1 - \tfrac{1}{3}S(t)]\}/(1+R), \quad (4)$$

where $S(t)$ is the deuteron form factor calculated from the Hulthén wave function, and R is the ratio of flip to nonflip contributions to the cross section. The factor 0.97 is a correction for Glauber shadowing. R must be zero at $t = 0$, and previous analyses have assumed $R = 0$ throughout the low-t region where the exclusion-principle suppression is important. The dashed curve in Fig. 1(c) shows $f(t)$ for $R = 0$. As described below, fits by the t dependence of the cross section suggest that at small t $R \approx 14|t|$, and we used this assumption to correct the data. The correction is listed in Table I and is shown as the solid curve in Fig. 1(c). As shown by the figure, the measured cross-section ratio between Reactions (2) and (1) is consistent with either choice of R.

The results are shown in Table I and Fig. 2. The K^- points were obtained by averaging the data from Reactions (1) and (2), with roughly $\frac{2}{3}$ of the events coming from hydrogen. Figure 1(d) shows the K^+-to-K^- ratios versus $(-t)^{1/2}$ for the three momenta. The data are consistent with a value of 1.35 independent of s and t. The ratios of cross sections integrated from $-t = 0$ to 0.5 GeV^2 are 1.49 ± 0.13, 1.37 ± 0.08, and 1.28 ± 0.09 at 3, 4, and 6 GeV/c, respectively.

The solid curves in Fig. 2 are fits with

$$d\sigma/dt = [a_0 J_0^2(r(-t)^{1/2}) + a_1 J_1^2(r(-t)^{1/2})]e^{Bt} \quad (5)$$

with r fixed at 0.8 fm (4.05 GeV^{-1}). This form is suggested by strong-absorption models[5] with the Bessel functions J_0 and J_1 describing the nonflip and the flip amplitudes, respectively. As t approaches zero, the flip-to-nonflip ratio approaches $R = R_0|t|$ with R_0 a constant. The six fits were made from 0 to 1 GeV^2 and have a total χ^2 of 49 for 42 degrees of freedom; changing r by ± 0.1 fm increases χ^2 by about 12 and changes R_0 by typically 2 GeV^{-2}.

The dashed curves in Fig. 2 are fits with

$$d\sigma/dt = (a_0 + a_1 t)e^{Bt}. \quad (6)$$

The χ^2's for these fits are also quite reasonable.

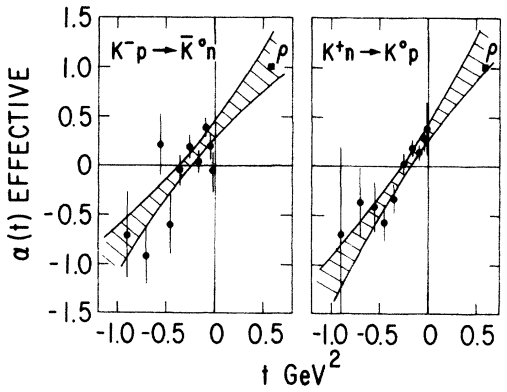

FIG. 3. Effective trajectories derived from the energy dependence of the results from this experiment. The shaded regions show the ± 1-standard-deviation uncertainties in the linear fits.

For both reactions our total cross sections are consistent with a $p^{-1.9}$ dependence. This result differs somewhat from the trends seen previously[6] which indicated a steeper falloff the K^+ reaction than for the K^- one.

The energy dependence of the differential cross sections was parametrized as

$$d\sigma/dt = f(t)s^{2\alpha(t)-2}. \quad (7)$$

The resulting effective trajectories $\alpha(t)$ are shown in Fig. 3 together with straight-line fits for the K^- and K^+ reactions,

$$\alpha^-(t) = (0.34 \pm 0.08) + (1.20 \pm 0.29)t, \quad (8)$$

$$\alpha^+(t) = (0.33 \pm 0.08) + (1.50 \pm 0.30)t. \quad (9)$$

The two fits are compatible with one another, showing the similarity of the energy dependences of the two reactions. Although both straight-line fits pass within 1 standard deviation of the ρ meson, the intercepts of 0.34 are lower than generally taken for the ρ trajectory, and $\alpha(t)$ crosses zero near $-t = 0.25$ GeV^2 instead of the nominal 0.6 GeV^2.

The spectrometer was designed and constructed in collaboration with I. Ambats, A. Lesnik, D. R. Rust, C. E. W. Ward, and D. D. Yovanovitch. R. Diaz, L. Filips, and E. Walschon were instrumental in the construction and maintenance of the spectrometer.

*Work supported by the U. S. Atomic Energy Commission.

†Present address: National Accelerator Laboratory, Batavia, Ill. 60510.

[1]D. S. Ayres, in *Proceedings of the International Conference on Instrumentation for High Energy Physics, Frascati, Italy, 1973,* edited by S. Stipcich (Laboratori Nazionali del Comitato Nazionale per l'Energia Nucleare, Frascati, Italy, 1973), p. 665; A. J. Pawlicki *et al.*, Phys. Rev. Lett. 31, 665 (1973); I. Ambats *et al.*, Phys. Rev. D (to be published).

[2]V. Barger and D. Cline, Phys. Rev. 156, 1522 (1967); D. Cline *et al.*, Phys. Rev. Lett. 23, 1318 (1969); D. Cline and J. Matos, Nucl. Phys. B37, 161 (1972); K.-W. Lai and J. Louie, Nucl. Phys. B19, 205 (1970).

[3]While the losses were quite small for $-t \lesssim 0.4$ GeV^2, they became substantial at large t, for example, a 22% loss at $-t = 0.9$ GeV^2 at 6 GeV/c.

[4]P. Fleury, in *Methods of Subnuclear Physics,* edited by M. Nikolic (Gordon and Breach, New York, 1968), Vol. II, p. 541.

[5]M. Ross *et al.*, Nucl. Phys. B23, 269 (1970); H. Harari, Ann. Phys. (New York) 63, 432 (1971); G. Berlad *et al.*, Lett. Nuovo Cimento 1, 339 (1971); Y. Matsumoto and S. Minami, Lett. Nuovo Cimento 3, 590 (1972).

[6]See for example G. Dehm *et al.*, Nucl. Phys. B60, 493 (1973).